Proceedings of the 9th International and 49th National Conference on Fluid Mechanics and Fluid Power (FMFP)
December 14-16, 2022, IIT Roorkee, Roorkee-247667, Uttarakhand, India

FMFP2022–XX–YYY

Planar Laser-Induced Fluorescence (PLIF) Studies on a High-frequency Pulsed Co-Axial Injector Flowfield

John T Solomon[1], Rhys Lockyer[2], Philip Kreth[3]

[1,2]Department of Mechanical Engineering, Tuskegee University, Alabama, USA
[3]Department of Mechanical, Aerospace, and Biomedical Engineering, University of Tennessee Space Institute, Tennessee, USA

ABSTRACT

Effective mixing in supersonic and hypersonic flow conditions is critical for developing next-generation high-speed air-breathing transport systems. Efficient fuel mixing with fast-moving air leads to a better economy and fewer pollutants. Ultimately the mixing is a molecular diffusion problem. However, the macroscopic phenomena, such as entrainment and vorticity dynamics resulting from the shear layer instabilities of the mixing fluids, play a significant role in the overall efficiency of the process. This paper studies a novel, co-axial injector system integrated with a high-frequency microjet actuator operating at 15.5 kHz for improving mixing in extreme flow conditions. This co-flow system consists of a high-frequency supersonic actuation air jet at the inner core that provides large mean and fluctuating velocity profiles in the shear layers of a fluid stream injected surrounding the core through an annular nozzle. The high-frequency streamwise vortices and shockwaves tailored to the mean flow significantly enhanced supersonic flow mixing between the fluids compared to a steady co-axial configuration operating at the same input pressure. This paper reports the flow mixing characteristics of the injection system captured using planar laser-induced fluorescence (PLIF).

Keywords: High-speed flow mixing, flow control, actuator, pulsed co-axial flow, PLIF

1. INTRODUCTION

High-speed air-breathing combustors require effective fuel mixing with a fast-moving oxidizer for efficient operation. A co-axial jet configuration is a simple and effective mixing method in which fluids flowing separately through the inner core and the annular space meet at the exit plane of the nozzle assembly. For example, in applications like a gas turbine or combustion chamber of a rocket engine, these fluids could be oxidizers, such as gaseous or liquid oxygen, and fuel in its liquid or gaseous phase. Effective and controlled mixing can lead to higher combustion efficacy, longer life, reduced combustor size, stable operations, and fewer emissions/pollutants. Although the mixing ultimately happens at the molecular level, active flow control techniques can tailor the flow dynamics at micro and macro scales in favor of rapid diffusion at the molecular level [1, 2].

The tiny convective time scale (order of milliseconds) associated with hypersonic flow systems demands effective fuel injection techniques for their efficient and stable operations. There is a need for robust flow control actuators to enhance microscale mixing at high-speed and positively alter the macroscopic phenomena involved. The entrainment and vorticity dynamics resulting from the shear layer instability modification are expected to play a significant role in the overall efficiency of the mixing process. Passive methods proposed for shear layer modifications use flush mounted or intrusive injectors to generate streamwise, counter-rotating vortices for rapid nearfield mixing of the incoming air and fuel [3]. Beyond the classical passive co-axial configuration, a few studies explore active schemes such as powered resonance tubes (PRT) or Hartmann-Sprenger tubes as an option to excite the shear layer of the mixing fluids at high frequency for improved mixing characteristics [4].

2. PULSED INJECTOR DESIGN AND EXPERIMENTAL METHODS

The current paper presents experimental studies on the flow mixing characteristics of a high-frequency co-axial injector configuration, as shown in Fig. 1. This design intends to tailor the instabilities of an injected co-flowing fluid using a pulsed supersonic air jet operating at 15.5 kHz with tuning bandwidth of $\pm$5 kHz. The injector assembly shown in Fig. 1 has three major components: 1) an under-expanded source jet from a steel tube of 1.5 mm diameter enters 2) an injector assembly made of three plates with internal cavities fabricated with the desired cavity volume of 20.3 mm^3, and 3) another steel tube (1 mm ID, 1.5 mm OD) that allows pulsed jet flows out of the cavities, and 4) a separate fluid passage that opens up around the 1 mm steel tube through a circular orifice of 1.95 mm diameter forming an annular space at the exit of the assembly. This annular space forms a circular slit with a 1.5 *mm* radius and a thickness of 230 micrometers, as indicated in fig. 1. This co-axial annular orifice injects a steady fluid stream while the central steel tube exit a pulsed actuation air jet. Both the fluids meet co-axially at the exit plane of the assembly, as shown in fig 1. Fig. 1 also shows a representative schematic of the pulsed co-axial flowfield from the injector. We reported the design details of the injection system, flow characteristics measured using microschlieren techniques, and initial PLIF data in reference [5].

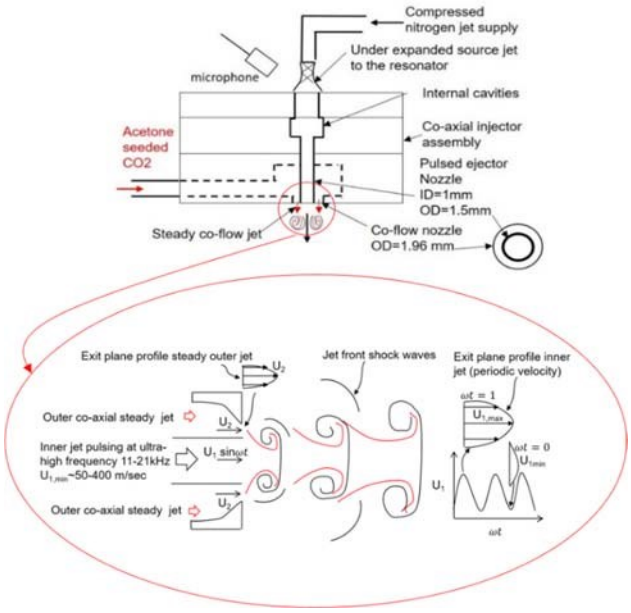

Figure 1: Schematic diagram of the pulsed co-axial injector and flowfield

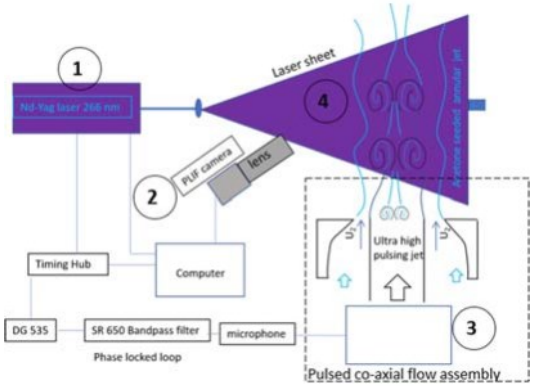

Figure 2: PLIF system and its various components used for this study

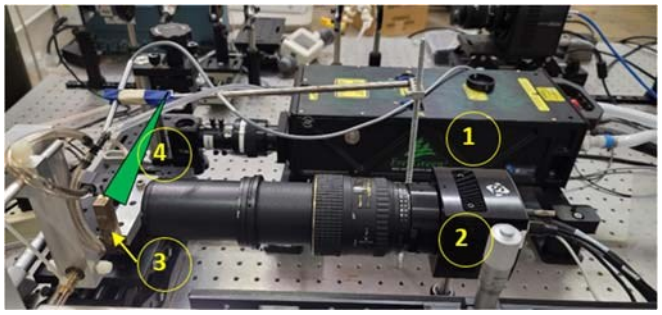

Figure 3: Photograph of PLIF experimental setup

2.1 Set up for planar laser-induced fluorescence (PLIF)

A schematic and a picture of the PLIF setup used for this study are shown in Fig. 2 and 3, respectively. The critical component of this setup is a Quantel EverGreen™ Nd-YAG dual pulsed laser with a choice of pulse energies up to 200 *mJ* at 532 nm and 30 *mJ* at 266 nm with a repetition rate of 15 Hz. PLIF experiments use laser pulses at 266*nm*. A Powerview™ LS-LCD camera (29 MP, 6600x4400), with high quantum efficiency, low noise with 1.8 frames/s, selectable 12-bit or 14-bit output, and 100 mm f/2.8 camera lens, acquires the images. An eight-channel digital laser pulse synchronizer with 250 *ps* resolution controls the laser pulses and the trigger for the camera. A UV optic periscope and adjustable laser sheet optics (LSO) with 266/532 mm AR coat create a thin laser sheet at an appropriate test plane in the flowfield generated by the pulsed co-axial assembly. A six jet oil droplet generator creates saturated acetone vapor in CO2 gas, which is used as the seed fluid stream for mixing experiments. The INSIGHT4G™ software is used for image acquisition and analysis.

2.2 Measurement of nearfield spectra of actuator flowfield

The unsteady spectra of the flowfield of the active nozzle assembly were measured using a GRAS™ 1⁄4-inch Free-Field Microphone with a sensitivity of 4 *mV/Pa*. National Instruments™ 9234, 24-bit, 51.2 kHz data-acquisition module acquires the microphone data using LabVIEW™. Fast Fourier transformation (FFT) of time series with 2048 data points and Hanning window with 50% overlap compute the acoustic spectra used in the analysis. The source jet pressure measurement has an uncertainty of 0.1 psi. The micro-gauge used for linear movements of the nozzle block, for varying the parameter *h/d*, has an uncertainty of 0.01 mm. A TSI™ Mass Flow Multi-Meter 5300-4 measures the flow rate of acetone seeded CO2 with 2% reading accuracy for measurements up to 300L/min.

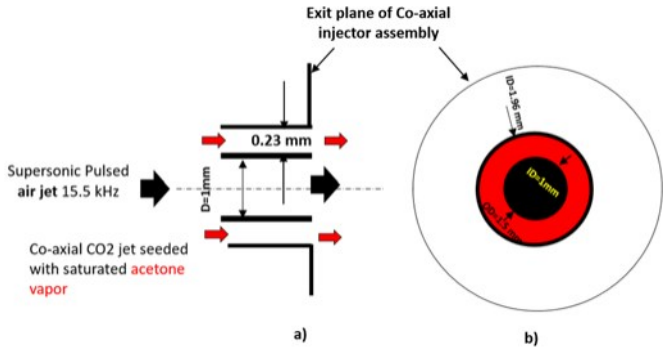

Figure 4: PLIF configuration for seeded annular jet and unseeded actuation jet

2.3 PLIF configuration for seeded annular jet and unseeded actuation jet

Figure 4 shows an exit plane view of the injector assembly where an annular stream of CO2 seeded with saturated acetone vapor interacts with the unseeded compressed nitrogen jet. The present experiments use CO2 at 8 psi and 4.7 lit/min flow rate. For a given annular exit area of 1.08 mm^2, this flow rate gives an estimated exit velocity of U2 ~50 m/sec for the seeded CO2 jet. The exit velocity U1 of pulsed jet varies 10-400m/sec during the cycle giving rise to a velocity ratio U1/U2=0.1-3.7.

3. RESULTS AND DISCUSSION

3.1 Frequency characterization of the pulsed co-axial assembly

In the present study, we chose three configurations for the preliminary experiments: 1) A seed jet alone, 2) a seeded jet with an actuation jet in a steady mode (without pulsing), and 3) a seeded jet with an actuation jet pulsing at 15.5 kHz. Figure 5 shows the microphone spectra of three cases. The pulsed co-axial flow shows a distinct frequency at 15.5 kHz, while the steady co-axial injection shows no specific tones in the spectra other than broadband noise. In steady actuation, energy is in broadband and is focused at 15.5 kHz for pulsed actuation. The spectra of the seed jet show low amplitude broadband noise indicating natural instabilities in the flow.

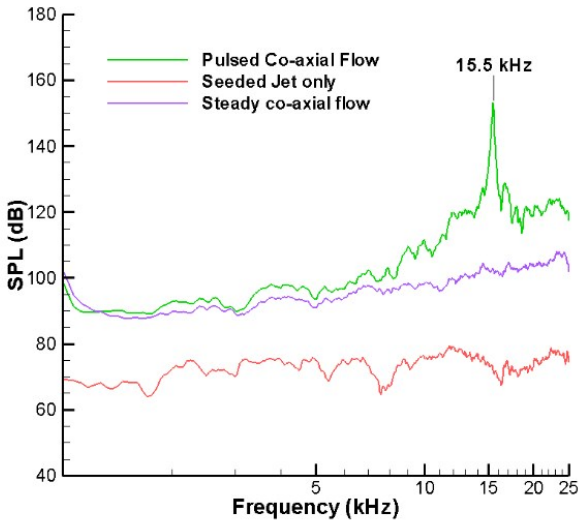

Figure 5: Spectra of three test cases i) seed jet only ii) steady co-axial flow iii) Pulsed co-axial flow at 15.5 kHz

3.2 Instantaneous images and mixing characteristics

Figure 6 shows a representative instantaneous PLIF image of test case 1, where acetone seeded CO2 stream is injected through the co-axial assembly without actuation jet, and the streamwise intensity profiles of this image at three selected locations as marked in the figure. Ideally, the saturated vapor exiting the nozzle fluoresces with maximum intensity (red color in PLIF image) and unseeded actuation jet and ambient air with zero intensity (black color in PLIF image). Assuming a linear variation between these two extreme values, the intensity of light fluoresce measured at a given location represents the local mixing of acetone with the surrounding unseeded streams. The high magnification optics and a high-resolution camera (27 MP) capture fine details of these high-speed microscale flows and their mixing characteristics in the PLIF images. For seed jet at 4.7 psi and 5 lit/min, images show the formation of a saturated core up to 10 diameters. The jet stream then seems to mix well with the ambient air further downstream by the natural diffusion mechanism. The PLIF profile at the center (blue curve) shows the distribution of seed particles in the streamwise direction. The red and green profiles show the streamwise distribution of seed particles at the top and bottom center locations of the co-axial stream, as indicated in fig. 6. These PLIF profiles represent the acetone concentration in the flow at various locations and provide information on its distribution in the flowfield.

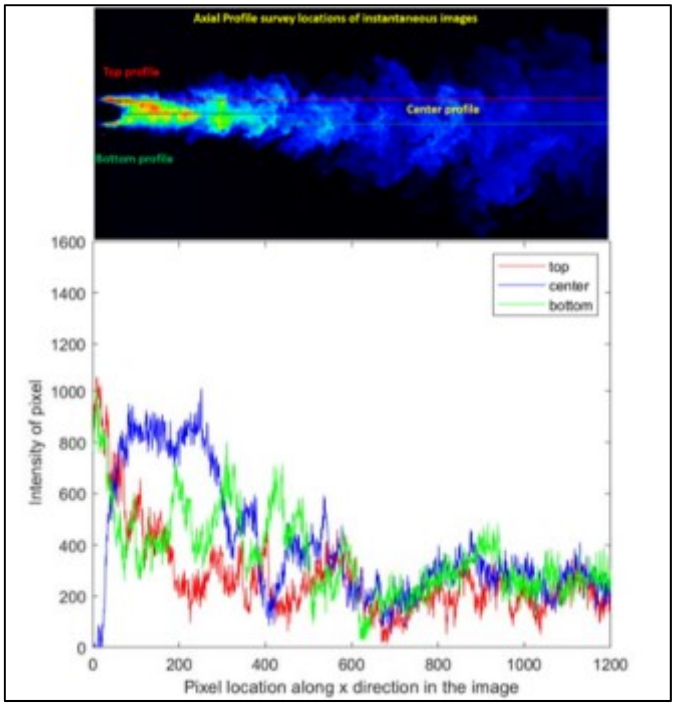

Figure 6: An instantaneous PLIF image and streamwise intensity profiles of seed jet at three locations marked in the figure

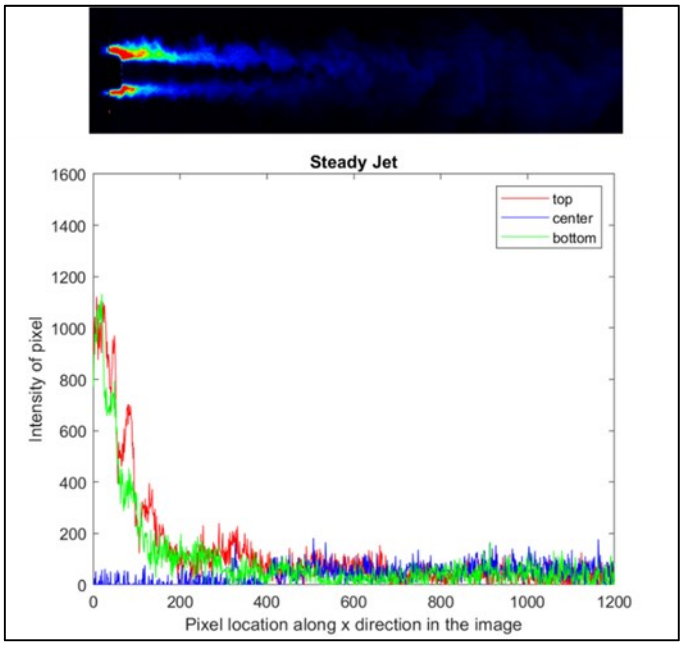

Figure 7: An instantaneous PLIF image and streamwise intensity profiles of steady co-axial flow at three locations

Figure 7 shows a representative instantaneous PLIF image

and intensity profiles of test case 2, where acetone seeded CO2 stream is injected through the co-axial assembly along with a steady actuation jet. The actuation jet is an underexpanded supersonic jet at 65 psi exiting a 1 mm nozzle located at the center of co-axial nozzle assembly as indicated in Fig. 3. This case represents a classical co-axial flow configuration. In this case, the jet core without seed particles appears to be extended up to 10*d* (*d*=1mm, the exit diameter of the actuation nozzle) and then weakens. These images reveal that the compressible shear layer of the steady under-expanded jet offers more resistance to the radial diffusion of co-axial seed particles into the jet core. The centerline survey also indicates that the diffusion of seed particles to the jet core is minimum for a steady actuation case.

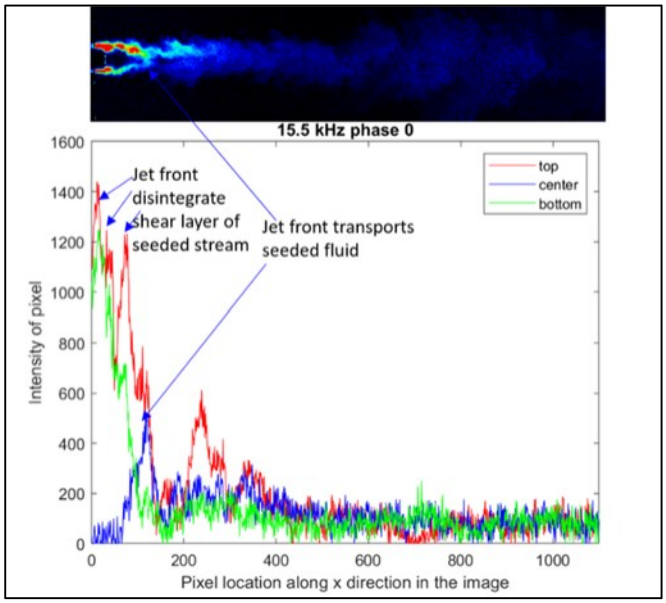

Figure 8: An instantaneous PLIF image and streamwise intensity profiles of the pulsed co-axial flow at three locations for phase 0°

Figure 8-10 shows representative phases of the *pulsed* co-axial actuation along with the intensity profiles when the actuator operates at 15.5 kHz. These figures correspond to phases 0°, 90°, 180°, and 270°, respectively. The pulsing action of the actuation jet creates high-frequency compressible vortexes in the flowfield in the same frequency range. This tailored vorticity created at the inner core of the seeded jet leads to the entrainment, mixing, and transportation of the seed jet to the actuator flow. The interfacial area of the vortex increases downstream, resulting in increased entrainment, diffusion, and mixing of the seeded CO2 jet with the actuation jet (N2) and the ambient air. As indicated in Fig. 8, at phase 0°, the evolving jet front and pulsed vortex disintegrate the shear layer saturated with acetone. This physical mechanism is also evident from the intensity profiles at the top and bottom locations. The intensity profile at the center (blue curve) shows a high concentration of seed particles close to the jet front which is moving with an estimated velocity of 200 m/sec. More details of velocity measurement using a phase-locked microschlieren imaging technique were reported in Solomon et al. [6]. Another phase 90°, shown in Fig. 9, indicates that the moving wavefront and shock wave created by the pulsed vortex transport seeded stream in the streamwise direction in favor of improved mixing of the seeded jet with the actuation jet and the ambient air. The highly oscillatory unsteady shear layer of the pulsing jet also enhances the diffusion of seed particles to the unseeded actuation jet.

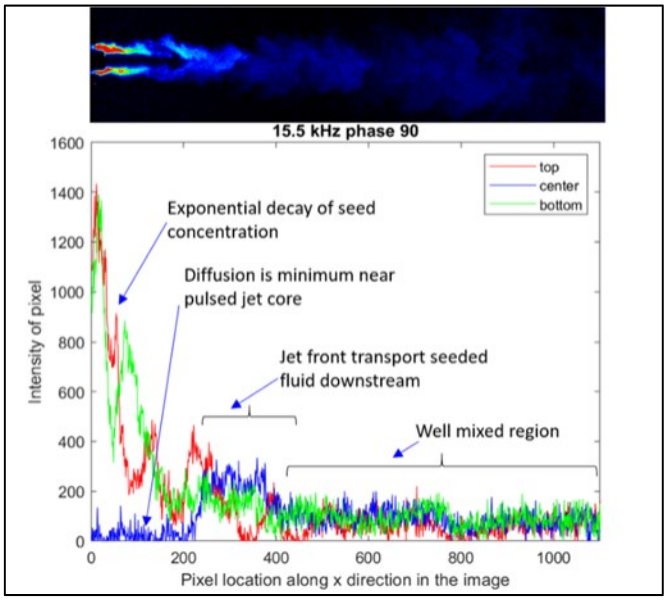

Figure 9: An instantaneous PLIF image and streamwise intensity profiles of the pulsed co-axial flow at three locations for phase 90°

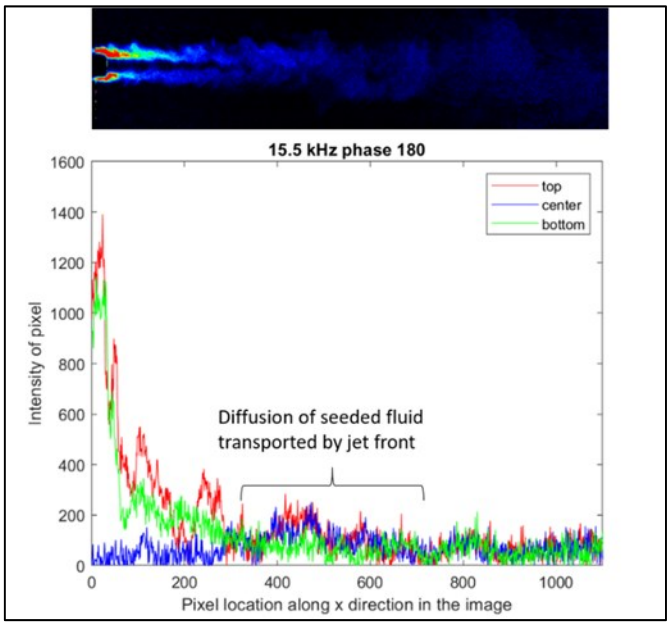

Figure 10: An instantaneous PLIF image and streamwise intensity profiles of the pulsed co-axial flow at three locations for phase 180°

The intensity profiles of phase 180° show gradual diffusion of the transported seeded stream with the unseeded actuation

jet. The intensity profiles in the final phase (270°) of pulsing indicate an increased acetone concentration at the center. The injected fluid converges to the center as the actuation jet velocity drops to a low subsonic range.

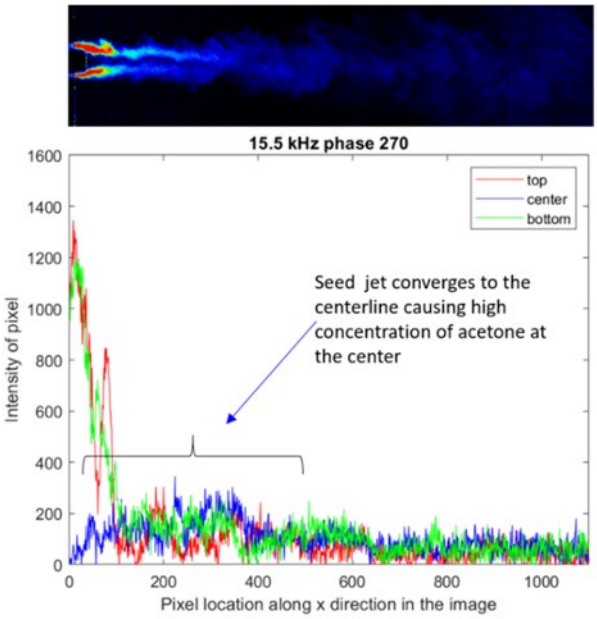

Figure 11: An instantaneous PLIF image and streamwise intensity profiles of the pulsed co-axial flow at three locations for phase 270°

The instantaneous PLIF images and the corresponding intensity profiles in figures 8-11 provide evidence of the enhanced mixing characteristics of this novel pulsed co-axial injector in comparison to a classical steady co-axial flow configuration shown in Fig. 7. To further estimate the efficacy of the pulsed scheme, 250 instantaneous PLIF images were acquired for each of this cases and its average intensity is calculated.

3.3 Averaged PLIF images and mixing characteristics

Figure 12 shows averaged images for each of the three cases calculated using 250 instantaneous PLIF images. Since each instantaneous image contains information on 4-5 cycles, the average image represents information on ~1000 cycles for the pulsed injection case. These averaged images provide a comprehensive view of all three cases' mixing characteristics and provide reasonably accurate quantitative estimates of the effectiveness of mixing effectiveness between the cases. The intensity of each pixel in the averaged PLIF image is proportional to the average acetone concentration around that elemental volume for the image sequences selected. An average of all pixel intensity estimates acetone concentration in a given field of view for a particular case. For the first case, seed jet alone, this number is 44.3. For the second case, when an unseeded steady actuation jet flows through the core, the acetone content we measure as average intensity in the same field of view changes due to fast relative motion between the streams. The average intensity of pixels measured for this case is 7.5. The same calculation for pulsed injections shows this average intensity value as 15.9. This calculation estimate that the mixing effectiveness of pulsed co-axial injection is 114% more than the steady co-axial injection. The enhanced mixing characteristics of the pulsed co-axial injection system attributes to the entrainment and growth of high-frequency vortex generated by the pulsed jets and through the shock wave diffusion through the interface of the seeded and unseeded flow downstream.

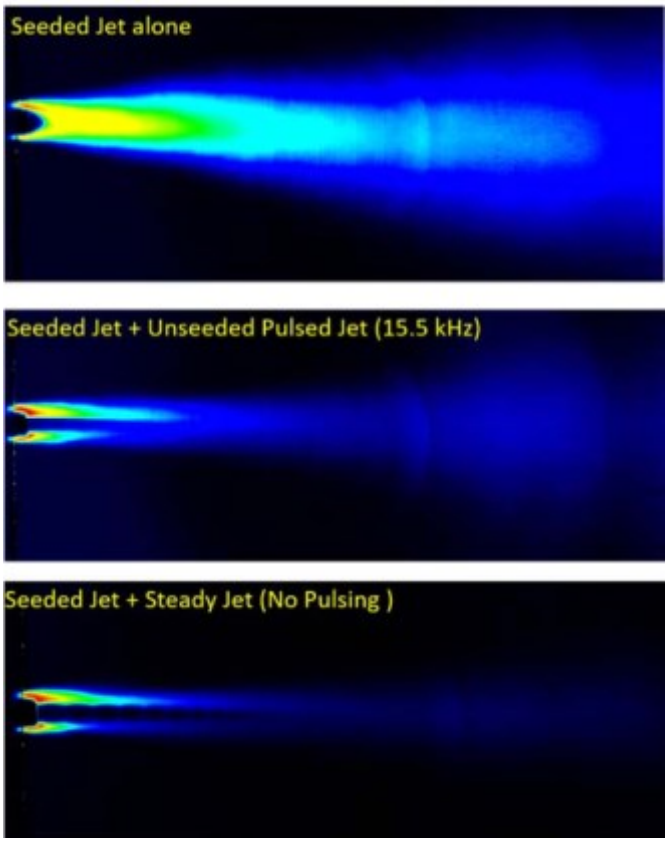

Figure 12: Average of 250 instantaneous PLIF images a) Seed jet alone b) Seed jet and steady actuation c) Seed jet and pulsed actuation at 15.5 kHz.

To better understand the mixing characteristics from the averaged images, we chose the same 3 locations on the exit of the injector assembly, as indicated in Fig. 6, and plotted the intensity profile along the streamwise direction. Fig. 13-15 represents the normalized intensity of the averaged image of the seed jet, steady jet, and pulsed jet at these 3 locations. These profiles show intensity varies continuously in the axial direction. A careful look at the profiles of the seed jet indicates the intensity at the top location is high compared to the bottom side due to the asymmetry at the exit. A slight downward inclination of the seeded jet core, as evident from Fig. 13, results in higher intensity values at the bottom location on the downstream side. Fig 14 and 15 show intensity profiles of steady co-axial flow and pulsed co-axial flow at three exit locations. The green curves indicate the centreline intensity in the axial direction. The mixing is minimum near the nozzle exit for steady co-axial flow (Fig. 14). It is evident from Fig. 15 that

the pulsed flow provides significantly enhanced mixing near the nozzle exit for the same pressure input to the co-axial assembly.

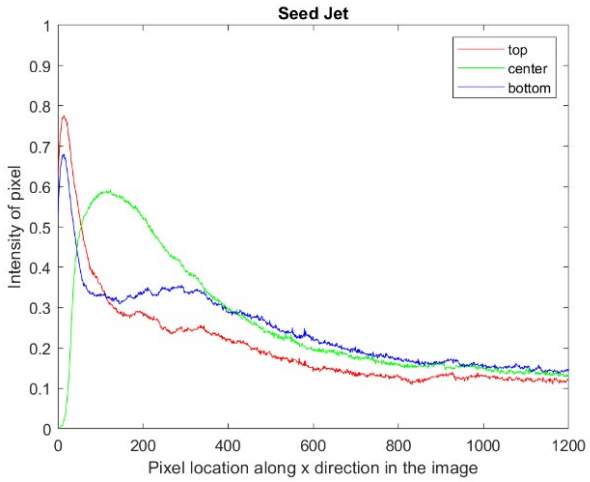

Figure 13: Normalized intensity profiles of averaged images of Seed jet in streamwise direction at three locations

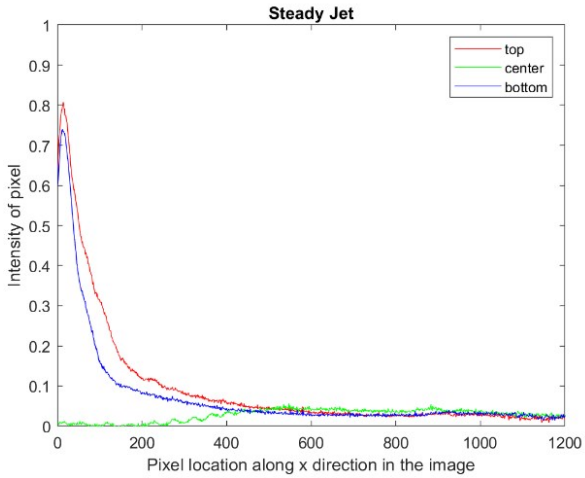

Figure 14: Normalized intensity profiles of averaged images of steady jet in streamwise direction three various locations

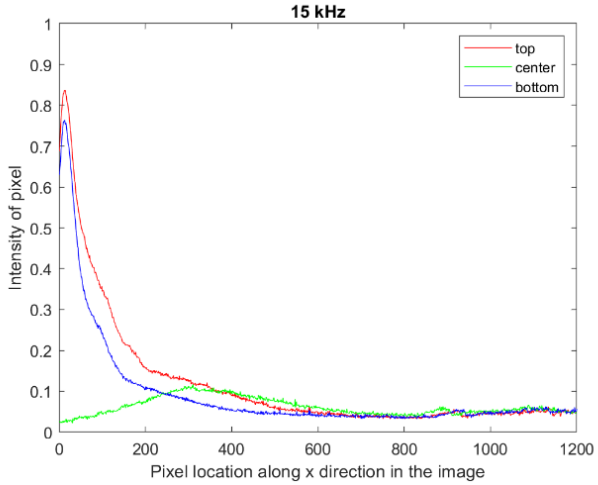

Figure 15: Normalized intensity profiles of averaged images of the pulsed jet in a streamwise direction at various locations

The high-frequency compressible air vortex generated in the injected flowfield and entrainment of the jet injected through the annular space cause significantly improved mixing between the two fast-moving fluids.

4. CONCLUSIONS

This paper reports an experimental study on an active, pulsed co-axial jet injection assembly integrated with high-frequency pulsed microjet actuators. The assembly steadily injects a fluid through an annular space around a 1 mm nozzle through which supersonic actuation air-jet flows out at a frequency of 15.5 kHz. The pulsed air jet develops a high-frequency compressible air vortex in the injected flowfield and entrainment of the jet injected through the annular space, causing significantly improved mixing between the two fast-moving fluids. The flowfield is analyzed using the planar laser-induced fluorescence (PLIF) technique, and PLIF uses saturated acetone introduced to the annular jet for quantitative mixing measurements. The experimental data shows that pulsed injection enhances mixing due to vortex entrainment, shock blasting through the fluid stream, vortex growth, and natural diffusion through the outer shear layers of the flow compared to a configuration with steady actuation. The PLIF image analysis estimates that pulsed injection significantly improved mixing by more than 100% compared to steady co-axial injection under the same injection pressure conditions. PIV experiments and parametric variations to these configurations are ongoing and will be reported in the future.

ACKNOWLEDGEMENTS

National Science Foundation supports this work through the Excellence in Research grant 1900177.

REFERENCES

[1] Davis, S. A. & Glezer, A., "Mixing Control of Fuel Jets Using Synthetic Jet Technology: Velocity Field Measurements," AIAA Paper 99-0447.

[2] Broadwell, J. E. and Mungal, M. G., "Large Scale Structures and Molecular Mixing," Physics Fluids, 1193-1206, 1991.

[3] Hsu, K., Carter, C. D., Gruber, M. R., and Tam, C., "Mixing Study of Strut Injectors in Supersonic Flows," AIAA Joint Propulsion Conference, AIAA Paper 2009-5226, 2009. doi:10.2514/6.2009-5226

[4] Hongbin, G., Zhi, L., Fei, L., Lihong, C., Shenglong, G., and Xinyu, C., "Characteristics of Supersonic Combustion with Hartmann-Sprenger Tube Aided Fuel Injection," AIAA Conference, AIAA Paper 2011-2326, 2011. doi:10.2514/6.2011-2326

[5] Solomon, J. T., Cairnes, K., Nayak, C., Jones, M. and Alexander, D. "Design and Characterization of Nozzle Injection Assemblies Integrated High-frequency Microactuators" AIAA Journal Vol. 56, No. 9, pp. 3436-3448, 2018.

[6] Solomon, J.T., Kreth, P.A., Lockyer, R., Jones, T., "High- Frequency Pulsed Co-axial Injectors for High-Speed Flow Mixing and Control, AIAA-3926, AVIATION 2022.